ELSEVIER

Remote Sensing of Environment 76 (2001) 283–297

Remote Sensing of Environment

www.elsevier.com/locate/rse

Laser altimeter canopy height profiles Methods and validation for closed-canopy, broadleaf forests

D.J. Harding[a,*], M.A. Lefsky[b], G.G. Parker[c], J.B. Blair[a]

[a]*Laboratory for Terrestrial Physics, NASA Goddard Space Flight Center, Mail Code 924, Greenbelt, MD 20771, USA*
[b]*USDA Forest Service, Forest Sciences Laboratory, Pacific Northwest Research Station, Corvalis, OR 97331, USA*
[c]*Smithsonian Environmental Research Center, PO Box 28, Edgewater, MD 21037, USA*

Received 16 December 1999; accepted 7 November 2000

Abstract

Waveform-recording laser altimeter observations of vegetated landscapes provide a time-resolved measure of laser pulse backscatter energy from canopy surfaces and the underlying ground. Airborne laser altimeter waveform data was acquired using the Scanning Lidar Imager of Canopies by Echo Recovery (SLICER) for a successional sequence of four, closed-canopy, deciduous forest stands in eastern Maryland. The four stands were selected so as to include a range of canopy structures of importance to forest ecosystem function, including variation in the height and roughness of the outermost canopy surface and the vertical organization of canopy stories and gaps. The character of the SLICER backscatter signal is described and a method is developed that accounts for occlusion of the laser energy by canopy surfaces, transforming the backscatter signal to a canopy height profile (CHP) that quantitatively represents the relative vertical distribution of canopy surface area. The transformation applies increased weighting to the backscatter amplitude as a function of closure through the canopy and assumes a horizontally random distribution of the canopy components. SLICER CHPs, averaged over areas of overlap where altimeter ground tracks intersect, are shown to be highly reproducible. CHP transects across the four stands reveal spatial variations in vegetation, at the scale of the individual 10-m-diameter laser footprints, within and between stands. Averaged SLICER CHPs are compared to analogous height profile results derived from ground-based sightings to plant intercepts measured on plots within the four stands. The plots were located on the segments of the altimeter ground tracks from which averaged SLICER CHPs were derived, and the ground observations were acquired within 2 weeks of the SLICER data acquisition to minimize temporal change. The differences in canopy structure between the four stands is similarly described by the SLICER and ground-based CHP results. However, a chi-square test of similarity documents differences that are statistically significant. The differences are discussed in terms of measurement properties that define the smoothness of the resulting CHPs and canopy properties that may vertically bias the CHP representations of canopy structure. The statistical differences are most likely due to the more noisy character of the ground-based CHPs, especially high in the canopy where ground-based sightings are rare resulting in an underestimate of canopy surface area and height, and to departures from assumptions of canopy uniformity, particularly regarding lack of clumping and vertically constant canopy reflectance, which bias the CHPs. The results demonstrate that the SLICER observations reliably provide a measure of canopy structure that reveals ecologically interesting structural variations such as those characterizing a successional sequence of closed-canopy, broadleaf forest stands. © 2001 Elsevier Science Inc. All rights reserved.

Keywords: Laser; Altimeter; Forest; Canopy; Structure; Height; Broadleaf; Lidar; Altimetry; Waveform; SLICER

1. Introduction

Characterization of canopy structure, defined as "the organization in space and time, including the position, extent, quantity, type and connectivity, of the aboveground components of vegetation" (Parker, 1995), is a major challenge in remote sensing, particularly for moderate- to high-biomass forests. Remote sensing approaches to measuring canopy structure (reviewed in Weishampel, Ranson, & Harding, 1996) depend strongly on the electromagnetic wavelength used and the sensor's spatial resolution. Passive, visible to mid-infrared optical sensors rely on solar illumination reflected mostly from the outer canopy surface. The intensity of the reflected signal is dependent on numerous, intermixed factors some of which relate to structure (i.e.,

* Corresponding author. Tel.: +1-301-614-6503; fax: +1-301-614-6522.
E-mail addresses: harding@denali.gsfc.nasa.gov (D.J. Harding), lefsky@fsl.orst.edu (M.A. Lefsky), parker@serc.si.edu (G.G. Parker), bryan@eib1.gsfc.nasa.gov (J.B. Blair).

0034-4257/01/$ – see front matter © 2001 Elsevier Science Inc. All rights reserved.
PII: S0034-4257(00)00210-8

composition, geometry, and density of canopy components) and some of which are unrelated (background composition, solar illumination angle, sensor view angle, and atmospheric transmittance). These sensors have been found to be insensitive to changes in biophysical parameters such as leaf area index (LAI) and biomass for moderately high to high-biomass systems, with useful results applying only to the lower half of the range over which these parameters vary (e.g., Chen & Cihlar, 1996; Lathrop & Pierce, 1991; Nemani, Pierce, Running, & Band, 1993; Sader & Joyce, 1990; Spanner, Peterson, & Running, 1990).

The longer wavelengths used by active synthetic aperture radar (SAR) polarimetry systems enable remote sampling of structure throughout a greater depth of vegetation canopies (Ulaby, Moore, & Fung, 1986). The intensity and polarization of the reflected radar signal are related to structural attributes of the canopy, but as a function of complex, wavelength-dependent scattering interactions with foliage, branches, trunks, and the ground (e.g., Sun & Ranson, 1995). In addition, like passive optical systems, radar polarimetry is insensitive to biophysical parameters at moderate- to high-biomass levels (e.g., Dobson et al., 1995; Imhoff, 1995; Le Toan, Beaudoin, Riom, & Guyon, 1992; Ranson, Sun, Weishampel, & Knox, 1997). Active SAR interferometry offers a potentially powerful new method to remotely estimate canopy height characteristics. Whereas SAR polarimetry is primarily sensitive to the shape and orientation of canopy components, SAR interferometry is primarily sensitive to the spatial distribution of radar scattering elements within the canopy (Treuhaft & Moghaddam, 1998). However, interferometry methods to date have depended on assumptions about, or independent knowledge of, canopy structure and/or ground topography in order to derive vegetation height information from the interferometric phase data (Askne, Dammert, Ulander, & Smith, 1997; Cloude & Papathanassiou, 1998; Dammert & Askne, 1998; Hagberg, Ulander, & Askne, 1995; Treuhaft, Madsen, Moghaddam, & Vanzyl, 1996).

A new class of instruments, referred to here as waveform-recording laser altimeters (Blair, Coyle, Bufton, & Harding, 1994; Blair, Rabine, & Hofton, 1999; Bufton, 1989; Bufton et al., 1991; Garvin et al., 1998), have demonstrated a potential to greatly improve remotely sensed estimates of important aspects of canopy structure. These devices expand upon the capability of traditional laser altimeters, which measure a single or several discrete ranges to a target, by digitizing the amplitude of the laser backscatter energy with very high temporal resolution. This waveform approach yields a measure of the height distribution of illuminated surfaces within the laser footprint. Aldred and Bonner (1985) described the first application of a waveform-recording laser altimeter in a study of forest canopies. They evaluated the performance of a laser system developed for bathymetric water depth sounding in order to assess its ability to determine stand height, closure, and type (hardwood, softwood, or mixed) for temperate forest stands in eastern Canada. Nilsson (1996) evaluated a similar bathymetric sounding system's measurement of mean height for pine stands in Sweden. He also showed that a prediction based on laser backscatter duration and amplitude was linearly correlated with stand volume up to the maximum volume observed (260 m^3/ha). Blair et al. (1994) implemented the first waveform-recording laser altimeter specifically designed to measure canopy structure by upgrading an instrument developed by Bufton et al. (1991). The profiling system described by Blair et al. was subsequently modified to incorporate a cross-track scanning capability, resulting in an instrument referred to as the Scanning Lidar Imager of Canopies by Echo Recovery (SLICER). Recent work has demonstrated that SLICER waveforms can be used to accurately predict the total biomass of specific stands (Lefsky, 1997; Lefsky, Harding, Cohen, Parker, & Shugart, 1999; Means et al., 1999), the variability of forest structure (Lefsky, Cohen, Harding, & Parker, in review; Lefsky, Cohen, et al., 1999), and light transmittance through forest canopies (Parker, Lefsky, & Harding, 2001) over a large range of biomass. SLICER waveforms have also been used to document multifractal spatial variations in longleaf pine stands (Drake & Weishampel, 2000).

2. Objectives

The objectives of this paper are to describe and validate a method that characterizes canopy structure using height profiles derived from SLICER waveforms. Specifically, we (1) describe the character of the raw SLICER backscatter signal, (2) present a method for transforming the raw signal into a canopy height profile (CHP) that quantitatively represents the vertical distribution of canopy components, (3) assess whether the measurements reveal, reproducibly, ecologically interesting variation in vegetation structure, (4) test the similarity of the derived canopy height data to analogous measurements made from the ground in closed-canopy, broadleaf forest stands, and (5) evaluate possible sources of differences in the SLICER and field derived CHPs.

Although this description and validation of CHPs is based on the use of SLICER data, the basic elements of the CHP method can be applied to any canopy laser altimeter waveform data including that acquired by the airborne Laser Vegetation Imaging Sensor (LVIS) and to be acquired by the spaceborne Vegetation Canopy Lidar (VCL). LVIS is a wide-swath, mapping system that has superceded SLICER (Blair, Rabine, & Hofton, 1999; Weishampel, Blair, Knox, Dubayah, & Clark, 2000). VCL will sample canopy height and structure over several percent of the Earth's land surface between $\pm 67^\circ$ during its 18 month mission (Dubayah et al., 1997).

We seek a remote measurement of canopy structure that is rapid, reproducible, and has spatial resolution commen-

surate with the scale of structural variation because existing ground-based approaches are slow, inexact, or highly averaged spatially. For example, though the foliage height profile approach (MacArthur & Horn, 1969) provides valuable information on the spatially averaged vertical distribution of leaf area (e.g., Aber, 1979; Aber, Pastor, & Melillo, 1982; Brown & Parker, 1994; Hedman & Binkley, 1988; Parker, O'Neill, & Higman, 1989), it requires a large effort and is, therefore, usually only justifiable for whole-stand characterization.

3. Laser altimeter waveform concept

A laser altimeter waveform is a record of the amplitude of backscattered laser energy reflected from the Earth's surface (in the absence of clouds) as a function of time (Fig. 1). The return signal is recorded at very high temporal resolution, thus, providing a finely resolved measure of the vertical distribution of illuminated surface area within the footprint, including plant area throughout the vegetation canopy. Where laser energy penetrates to the canopy floor and is reflected back to the receiver, a measure of canopy height is obtained for that laser pulse from the travel time between canopy top and ground reflections. The intensity of the received backscatter return at a given depth in the canopy depends on the amount of laser illumination penetrating to that depth and on the reflectivity of the intercepted surfaces at the wavelength of the laser. Transmitted laser energy per unit area decreases with depth through the canopy due to occlusion (reflection and absorption) by plant area encountered higher in the canopy. In addition, because the spatial distribution of laser energy is not constant across a laser footprint, the horizontal organization of reflecting surfaces with respect to the laser energy spatial distribution affects the intensity of the return (Blair & Hofton, 1999). In summary, the time history of backscatter energy is a measure of the vertical distribution of illuminated surface area, projected in the direction of the laser vector, weighted by the reflectance of the surfaces at the monochromatic laser wavelength and the spatial distribution of laser energy across the footprint.

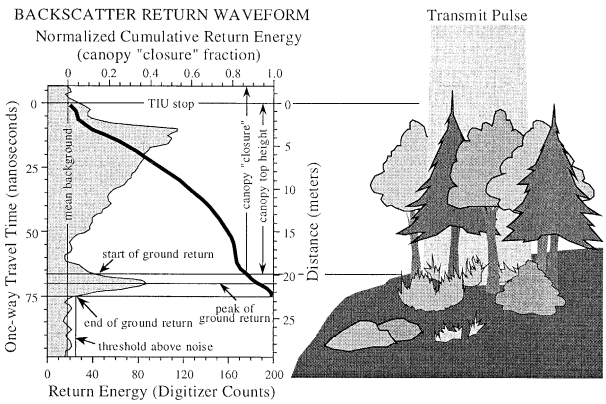

Fig. 1. Illustration of backscatter return energy as a function of travel time (gray-shaded distribution) for a single laser pulse, with the start, peak and end of the ground return indicated. Travel time is converted to distance based on the speed of light through a standard atmosphere, yielding canopy height from the distance between the highest detected canopy top (time interval unit (TIU) stop) and ground return start. The cumulative distribution of return energy (solid curve), accumulated downward from the canopy top and normalized, is a measure of canopy closure (not corrected for differences in reflectance of the ground and canopy).

The received laser energy consists of returns due to single and multiple scattering events. Single scattering events consist of photons that encounter only one surface and are reflected directly back to the receiver at 0° phase angle (parallel illumination and view angles). Multiple scattering events are comprised of photons that encounter more than one surface before being reflected back to the receiver, as can be the case for laser energy that is transmitted through or forward scattered-off foliage and, subsequently, is reflected from another surface. Laser energy reflected from the ground consists of singly scattered photons, where a gap extends through the entire canopy to the ground in the direction of the transmit pulse, as well as some fraction of multiply scattered photons. The path for multiply scattered photons is longer than the straight-line path between instrument and target and, thus, those photons appear delayed in the waveform compared to singly scattered photons. The amount of delay depends on the distance between scattering events and is, thus, a function of clumping of the canopy elements.

The relative strength of the canopy and ground returns provides information on canopy closure. We use the term canopy closure to mean the fraction of plant area per unit area, projected along the direction of the transmitted laser pulse (one minus the gap fraction). The cumulative height distribution of canopy energy, normalized by the total return energy, is a relative measure of canopy closure as a function of height (Fig. 1). Independent knowledge of the average reflectance of the canopy and ground surfaces within the laser footprint is necessary to convert the cumulative distribution to an absolute measure of canopy closure. The cumulative distribution also makes the simplifying assumption that only single scattering events contribute to the return signal.

4. SLICER characteristics

The SLICER system records range to surfaces utilizing a laser transmitter, scan mechanism, receiver telescope, detector, timing electronics, waveform digitizer, and an instrument control and data collection system. The laser transmitter operates in the near infrared (NIR) at 1064 nm. The system is augmented by an inertial navigation system for precise determination of laser beam pointing, GPS receivers for differential, kinematic determination of aircraft position, and coaligned, time-stamped video for documentation of the ground track. Integration of the ranging data with

laser beam pointing and aircraft position yields a position and elevation for each laser pulse return with respect to a geodetic reference frame (Hofton, Blair, et al., 2000; Vaughn, Bufton, Krabill, & Rabine, 1996), so the data can directly correlated with georeferenced ground observations and remote sensing images. Details of the instrument and its operating characteristics are described in Harding, Blair, Rabine, & Still (2000).

Several aspects of the SLICER design make it a powerful tool for characterizing canopy vertical structure. The combination of a very narrow transmit pulse and a high-speed detector results in vertical resolution of approximately two-thirds of a meter, allowing closely spaced canopy layers and the underlying ground within each footprint to be distinguished. Use of a very high-speed digitizer to sample the detector output results in a nonaliased waveform record of backscatter energy that has extremely good vertical sampling (11.12 cm), necessary for full analysis of waveform structure. SLICER employs a high power laser that enables flight altitudes up to 8 km. A nominal flight altitude of 5 km and laser divergence of 2 mrad yields circular footprints 10 m in diameter. The canopy in these large footprints typically contains some openings at nadir to the ground, thus, consistently yielding a ground return and enabling a measure of vegetation height for each laser pulse. Adjacent footprints are typically contiguous, or even overlapping, and, thus, fully illuminate the canopy, providing a measure of average canopy structure that avoids the sampling bias inherent to the spaced data points of small footprint altimeters. By scanning the laser footprints across the flight path, a narrow swath results, which provides cross- and along-track data from which information on canopy heterogeneity and ground slope beneath the canopy can be inferred.

Several implications of the instrument characteristics are significant for proper use of the SLICER data. First, the spatial pattern of canopy sampling is uneven due to the pattern of circular, approximately contiguous laser footprints that each have a radial, Gaussian distribution of laser energy (Fig. 2). Second, the amplitudes of waveforms cannot be compared in an absolute sense because the measure of received energy is uncalibrated, varying in time and across the swath. Thus, the waveform is most properly used as a relative measure of the height distribution of backscattered energy within an individual footprint. Third, because SLICER utilizes a threshold detection scheme to define the range to the first detected target within a footprint, detection of the canopy top requires that sufficient backscatter energy be received and, therefore, depends on the geometry and reflectivity of the outer canopy. For example, narrow, erect conifer tips with relatively dark needles at NIR wavelengths are less easily detected than a concentration of NIR-bright deciduous leaves forming a well-defined, umbrella-like crown top. SLICER measurements of canopy height can be biased low by varying amounts compared to the outermost canopy surface and, thus, stand-specific calibrations of canopy height measurements are necessary.

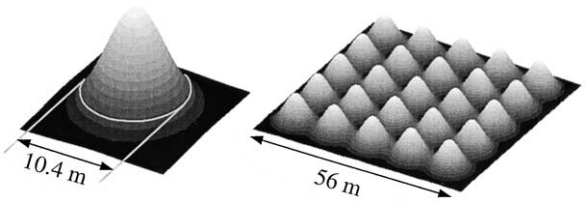

Fig. 2. Perspective views of laser pulse Gaussian energy distribution for a single SLICER footprint (left) and a 5×5 array of footprints (right). The average footprint diameter in this study, defined where the energy decreases to $1/e^2$ (i.e., 13.5%) of the peak (gray circle, left), is 10.4 m based on a 2-mrad divergence of the transmitted laser pulse and the average ranging distance to the ground. The 5×5 array is composed of footprints with cross-track and along-track spacing equal to the footprint diameter. In this ideal case, the energy minima between footprints decrease to 8% of the peaks.

5. Experiment description

Derivation of CHPs from laser altimeter waveforms is based on transformation of the raw backscatter record using a method that accounts for the occlusion effect inherent to the range measurements. We assess SLICER-derived CHPs by comparing them with ground-based, manually observed height profiles for four forest stands of diverse structure. The ground-based approach is only appropriate for measurement of spatially averaged characterizations of whole-stand vertical structure. Therefore, the validation is based on comparison of whole-stand structure using coincident ground and laser waveform data averaged over the same spatial scale. This validation is straightforward in that it compares the same type of observations (i.e., distributions of intercept distance). Furthermore, the observations from both SLICER and the ground are transformed to height profiles of vertical structure using methodologies that similarly account for the occlusion effect common to both sets of data.

5.1. Study sites

Work was carried out in four closed-canopy stands of very different vertical structure that represent stages in a successional sequence of the "tulip poplar" association, a mixed deciduous forest with overstory dominated by *Liriodendron tulipifera* (Brush, Lenk, & Smith, 1980; Eyre, 1980). Specific stands were selected that have been the subject of previous studies of forest development and structure (e.g., Brown & Parker, 1994; Parker et al., 1989). Three stands are within 5 km of each other, at the Smithsonian Environmental Research Center (SERC, 38°53′N, 76°33′W), about 10 km SSE of Annapolis, MD on the western shore of Chesapeake Bay. They include a young stand with a narrow unimodal canopy, an intermediate-aged stand with a broad unimodal canopy, and a mature stand with a bimodal vertical leaf area structure, referred to

Table 1
Summary of stand structure for the four study sites used for SLICER validation

Characteristic	Site			
	Young	Intermediate	Mature	Old-growth
Area sampled (ha)	0.06	0.1	0.5	0.3
Estimated age (years)	13	41	99	234
Stem density (stems/ha)	5683	840	1187	1373
Basal area (m^2/ha)	34.7	39.7	34.7	60.9
Highest leaf (m)	17	30	36	41
Number of woody species	9	14	19	22
Leaf area index (m^2/m^2)	4.21	5.16	5.26	6.77

as "crnb," "kph4," and "twrc," respectively, in Brown and Parker (1994). The intermediate age and mature stands are located within a forest at SERC for which a 600×600 m stem map has been produced that is georeferenced to Maryland State Plane coordinates (Lefsky, Harding, et al., 1999). The fourth site is old-growth forest 20 km to the west (76°46′W, 38°54′N), known locally as the Belt Woods, which has a tall bimodal structure. Characteristics of each stand are summarized in Table 1.

5.2. SLICER data acquisition

SLICER data were acquired for the four study sites on September 7, 1995. The canopies were fully leaved at this time, with no senescence having yet occurred (Parker & Tibbs, in review). Using a GPS flight navigator, six lines, separated in heading by 60°, were flown across the SERC stem map centered on a meteorological flux tower. Aircraft roll caused local perturbations of the data ground tracks, up to several hundred meters off the flight track. One line each was flown across the young and old-growth stands. The accuracy of the SLICER footprint geolocation was established to be at the scale of the footprints by comparing altimeter elevation profiles to features within the georeferenced stem map having distinctive heights (flux tower, dominant crowns, gaps). The horizontal offset between the SLICER ground tracks and the SERC stem map reported, in Lefsky, Harding, et al. (1999) is thought to be due to a reference frame discrepancy introduced during separate transformations of the two data sets to the UTM projection. Those transformations were not used in this paper.

Transects of raw waveform return amplitudes were examined to identify segments of uniform backscatter character within each of the four study sites. For the intermediate-aged and mature sites within the SERC stem map grid, the field location of the uniform segments was established by converting footprint latitude and longitude, referenced to the WGS-84 ellipsoid, to grid coordinates, referenced to the Maryland State Plane system. Lacking field grids for the young and old-growth stands, the ground locations of the SLICER segments for these sites were established using the simultaneously acquired video images.

5.3. Ground data acquisition

The relative vertical distribution of plant area was measured within 2 weeks after the SLICER flight in each stand along the selected altimeter ground track segments using the method of MacArthur and Horn (1969), as modified by Aber (1978) and Parker et al. (1989). A telephoto lens calibrated to measure distances was used to generate a distribution of the heights of the nearest surface above the observer to within 1 m resolution. At each observation location, 15 interceptions, arrayed in a 3×5 grid inscribed on the telephoto lens, were recorded. A grid of observation locations was established to systematically sample across the width of the SLICER data swath (e.g., Fig. 3). The total number of interception observations was 615, 1020, 1260, and 1575 in the young, intermediate, mature, and old-growth sites, respectively, increasing as a function of stand height in order to provide an approximately equal number of observations per meter of height.

The interception observations for all foliage and woody surfaces were combined and transformed to yield a relative distribution of total plant area as a function of height (i.e., CHP). It is important to note that this method provides a relative plant area height distribution; it does not yield an absolute measure of total plant area (Brown & Parker, 1994). The transformation converts the distribution of intercept distances to the relative distribution of plant area by weighting the intercept to account for the effect of increasing occlusion with distance, following the Aber (1978) modification of the MacArthur and Horn (1969) method. The magnitude of the weighting increases with distances in a manner that depends on total gap fraction observed, defined by the proportion of clear-sky to total interception sightings. The weighting at a given distance is larger for canopies with smaller gap fraction. The gap fractions for these closed canopies were all small: young,

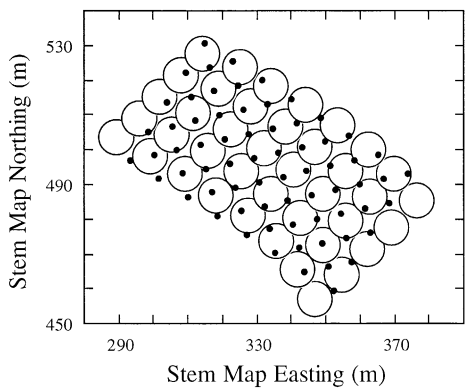

Fig. 3. Sampling geometry for the intermediate-age stand within the SERC stem map depicting the SLICER swath, composed of five cross-track footprints (open circles), and ground sampling grid (filled circles). The position of the SLICER footprints as shown with respect to the ground grid is illustrative; the relative position accuracy between the two data sets is approximately 10 m due to geolocation uncertainty.

intermediate, mature, and old-growth stands were 0.06, 0.05, 0.02, and 0.06, respectively.

6. Derivation of SLICER CHPs

To derive CHPs from the raw SLICER waveform distributions, we adapted the transformation method applied to the ground-based sightings. Assumptions regarding canopy uniformity inherent to the transformation of the ground data (Aber, 1978) also apply to the transformation of SLICER waveforms. The horizontal distribution of canopy components within a layer is assumed to be random with respect to layers above and below (i.e., a Poisson distribution with no horizontal clumping of canopy components). In addition, the leaf inclination distribution is assumed to be constant as a function of height so that the projected leaf area in the direction of observation is related in a constant way to total leaf area.

Several additional assumptions specific to laser altimeter waveforms must also be made. To obtain an equivalent parameter to clear-sky sightings, the proportion of ground return to canopy return signal strength is used. However, for this proportion to represent downward-viewed gap fraction, the ground return signal strength must be modified to account for any difference in the average reflectance at 0° phase angle of the ground and canopy at the laser wavelength. In most circumstances, this ratio between ground and canopy reflectance is not known at the scale of the laser footprints and a value must be estimated. Application of the method to waveforms also assumes that the reflectance of the canopy components is constant as a function of height. Whereas for the ground sightings, each canopy intercept counts equally in the resulting distribution, for waveforms, an equivalent surface area contributes greater return signal as reflectance increases. This assumption inherently implies that the ratio of woody to leafy surface area and the woody and leafy reflectance are constant as a function of height. Finally, it is assumed that multiple scattering does not contribute significantly to delayed signal in the waveform, because either the amount of multiply scattered photons received in the backscatter direction is small compared to singly scattered photons or the magnitude of any resulting delay is small.

Applying the above assumptions, a sequence of processing steps transforms the raw waveform into a CHP (Fig. 4). The steps consist of smoothing the signal, identifying the background noise level, differentiating the ground and canopy returns, adjusting the return amplitudes to account for differences in reflectance, computing a height distribution of canopy closure, and applying an occlusion transformation to yield a normalized height distribution of plant area. The following description, which expands upon and modifies the method reported in Lefsky (1997) and Lefsky, Cohen, et al. (1999), is specific to SLICER waveforms. However, the basic steps and underlying assumptions are applicable to any waveform-recording laser altimeter.

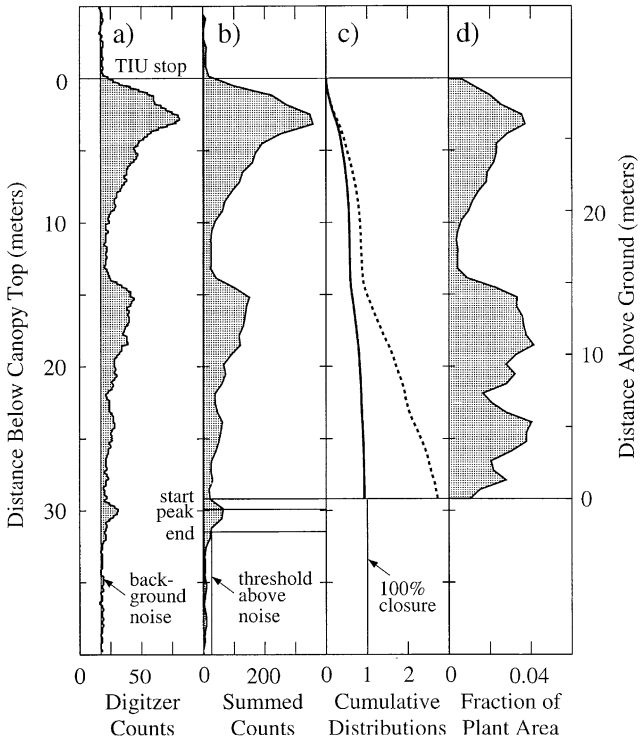

Fig. 4. Transformation steps converting a raw SLICER waveform to a canopy height profile: (a) raw waveform with 0.11-m sampling interval for a single laser pulse; (b) waveform above mean background noise summed to 0.66-m sampling interval, and start, peak, and end of the ground return identified; (c) cumulative distributions of canopy closure (solid), assuming ground reflectance that is half that of the canopy, and transformation to projected plant area (dashed) applying the MacArthur–Horn methodology; and (d) normalized, incremental distribution of plant area above ground.

To improve the signal-to-noise ratio of the waveform (Fig. 4a), six adjacent bins are summed, yielding a 66-cm vertical sampling, which is approximately equal to SLICER's vertical resolution. The mean and variance of the background noise are established using the final portion of the waveform, beyond any potential last ground return (a 61-m height interval downward from the canopy top was recorded in each waveform, which is significantly greater than the maximum height for the observed stands). The mean background noise is subtracted from the summed distribution yielding signal above the noise level (Fig. 4b). Negative results, where the variance in the noise causes the waveform signal to be less than the mean noise, are set to zero.

The ground reflection is identified by assuming that it is the last discrete return above noise. The end of the last return is defined as the latest signal above a threshold that is a multiple of the background noise variance (Fig. 4b). The peak of the last return is defined to be the first inflection in signal strength prior to the end of the last return, identified using its first derivative. The start of the last return cannot be uniquely identified from the raw distribution because backscatter return from low vegetation could be convolved

in time with the ground return. Therefore, the start of the last return is identified based on the width characteristics of the system impulse response. The impulse response is the theoretical signal recorded from a smooth and flat surface and depends on the convolved effects of pulse width and detector response. The SLICER impulse response is established from minimum-width returns from water surfaces. A ratio is determined for the impulse response between the width from the signal end to peak compared to the width from peak to start. The observed end-to-peak width of the last return is scaled by this ratio to define the start position of the last return. This method accounts for any pulse broadening of the last return due to slope or roughness of the ground within the footprint. More precise methods for identifying last returns (Carabajal et al., 1999; Hofton, Minster, & Blair, 2000) rely on fitting multiple Gaussian distributions to each waveform; this approach was not used because of the markedly non-Gaussian temporal character of the SLICER transmit pulse (Harding et al., 2000). After automated identification of the last returns, the results are interactively evaluated, and modified where necessary, by examining the raw waveform, with the last return identified, along with profile plots of last return start, peak, and end elevations. Anomalous variations in elevation or last return width, either along or across the SLICER swath, reveal improperly identified ground returns that are then manually corrected on the raw waveform.

The amplitude of the identified ground reflection (area under the curve above mean noise) is scaled to account for the difference between average canopy and ground NIR reflectance at 0° phase angle. For this work, the ground return amplitude was increased by a factor of 2 based on the assumption that the reflectance of the ground, dominantly comprised of leaf-litter with some bare soil and rare live foliage, was half that of the canopy. A factor of 2 was chosen based on typical NIR reflectance spectra of leaf-litter and soil vs. deciduous foliage. The results of this work are relatively insensitive to potential errors in this reflectance scaling factor, as described in the Discussion.

A cumulative height distribution for the canopy return is calculated, normalized by the adjusted total return (canopy + scaled ground), yielding a height distribution of canopy closure (Fig. 4c). The effect of occlusion is corrected by weighting this distribution by $[-\ln(1-\text{closure})]$ (Aber, 1978; MacArthur & Horn, 1969), transforming the result to a cumulative distribution of plant area projected in the direction of the laser beam (Fig. 4c). The cumulative distribution is normalized and converted to an incremental height distribution, yielding the CHP that depicts the fraction of total plant area per measurement interval (Fig. 4d). The height of the CHP intervals is referenced to the start of the ground return. Comparing Fig. 4a–d, one observes that signal at greater depths into the canopy is proportionally increased by the weighting that accounts for occlusion. This method of establishing the relative height distribution of plant area, depending only on the relative amplitude distribution within a single waveform, is consistent with the varying and uncalibrated relationship between waveform amplitude and received backscatter energy for SLICER (Harding et al., 2000). There is no dependence on absolute backscatter energy and no comparison of energy amplitude between laser shots is made.

7. Reproducibility of SLICER CHPs

To test the reproducibility of the SLICER-derived CHPs, the results at ground track intersections are compared for six locations within the SERC stem map (Fig. 5). This reproducibility test is an end-to-end check of the SLICER system, evaluating the integrated system components (instrumentation, geolocation methodology, and CHP processing algorithms). Five of the intersection areas occur entirely within the mature stand that has a bimodal vertical leaf area structure. The intersection of lines 1 and 2 is dominantly within the mature stand but partly includes the intermediate-age stand that has a broad, unimodal vertical structure. The CHPs for footprints within an overlap area for each flight line were averaged together, yielding an average CHP per line (Fig. 6).

Specific features of the CHPs at each intersection are consistently reproduced. Each intersection area yields a bimodal distribution, with overstory and understory modes, in which the height above the ground, width, peakedness, and amplitude of each mode, and the amplitude and height of the minimum between the modes (midcanopy gap) are reproduced. The maximum height of the CHPs agree to

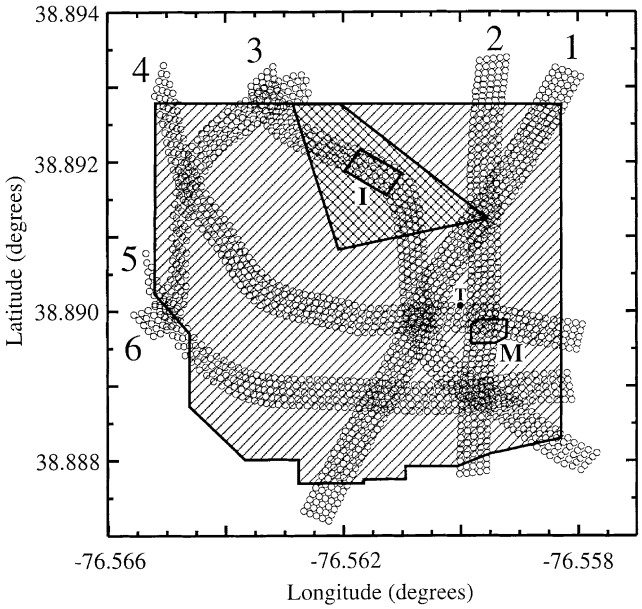

Fig. 5. Ground track map for the SLICER flight lines (numbered 1 to 6) across the SERC stem map comprised of intermediate-age (cross-hatched) and mature (diagonal pattern) stands, with the ground sampling plots outlined (I and M, respectively) and the location of the SLICER footprint on the flux tower indicated by the filled circle (T).

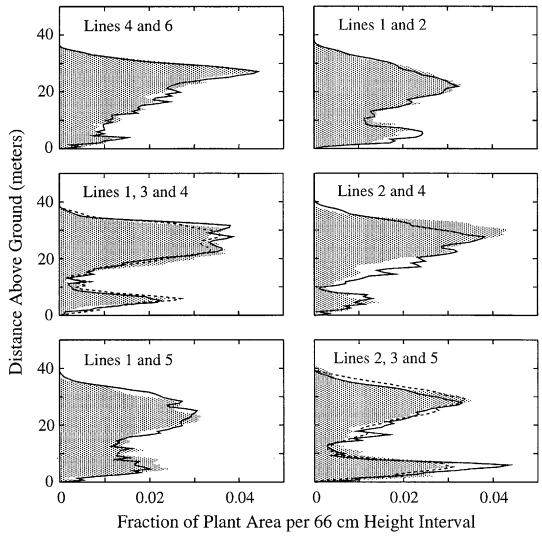

Fig. 6. SLICER average canopy height profiles per flight line (solid, shaded, and dashed distributions) from the areas of overlap at the ground track intersections within the SERC stem map.

within 1 m or better, and the initial slope of the distribution from the maximum height to the peak of the upper mode is very uniform. The initial slope is inferred to be a measure of the ruggedness of the outer canopy, with flatter slopes correspond to a more planar outer canopy. Discrepancies in initial slope and upper mode height and width between lines 2 and 4 are possibly due to footprints in this area of overlap that lacked any recognizable ground return, probably due to nearly complete or complete canopy closure. These footprints were excluded from the derivation of the average CHPs, possibly yielding CHPs representing slightly different areas.

Not only are the CHPs reproduced at each intersection; variations between intersections are also revealed. The maximum height, the initial slope, and the height, width, peakedness, and amplitude of the modes vary from location to location. The relative size of the lower modes compared to the upper modes markedly vary between locations, as does the amplitude of the minimum between the modes. The variations are greater than the differences between repeat CHPs at a single intersection location indicating that the variations are reproducibly detected. The spatial scale of CHP variation is revealed in transects across the four study sites depicting results for individual laser shots along a single, cross-track beam position within the SLICER swath (Fig. 7). The young site, with a very uniform, unimodal CHP structure, is a narrow stand bounded on the southwest by a riparian forest and on the northeast by a corn field, which had a mature, standing crop at the time of the SLICER flight (Fig. 7a). The intermediate-age stand has a uniform maximum height and, in general, consists of a relatively broad overstory and a minor to absent understory (Fig. 7b, derived from line 3 in Fig. 5). However, a 30-m-wide section within the middle of the stand consists of a uniformly distributed CHP throughout the height of the canopy. The ground sampling plot (gsp) includes both this segment and the more typical, broad overstory structure. The mature stand is, on the average, taller than the intermediate-age stand but has a more variable maximum height (Fig. 7b). The mature CHPs show a bimodal structure with a narrow overstory, a midcanopy gap, and a pronounced understory. The magnitude and depth of the understory varies spatially, consistent with the variable understory in the average CHPs at the intersection areas in the mature stand (Fig. 6). The old-growth stand is tall with a variable maximum height, a relatively narrow overstory, a broad midcanopy gap, and a pronounced but variable understory (Fig. 7c). Significant understory development occurs where 20- to 30-m-wide gaps are present in the overstory (at 280 and 350 m in Fig. 7c).

8. Comparison of SLICER and ground CHPs

The validity of the SLICER CHPs was assessed by comparing average SLICER and ground-based CHPs for the set of SLICER footprints that overlap with the ground sampling grids at the four study sites. A total of 16, 24, 12, and 79 footprints were used in the derivation of the average SLICER CHPs for the young, intermediate-age, mature, and old-growth stands, respectively. For each site, the waveforms were first summed for all the footprints, referenced in height to the start of the ground return, prior to computation of the average SLICER CHPs. The CHPs were computed with a 1-m vertical bin resolution to be comparable to the

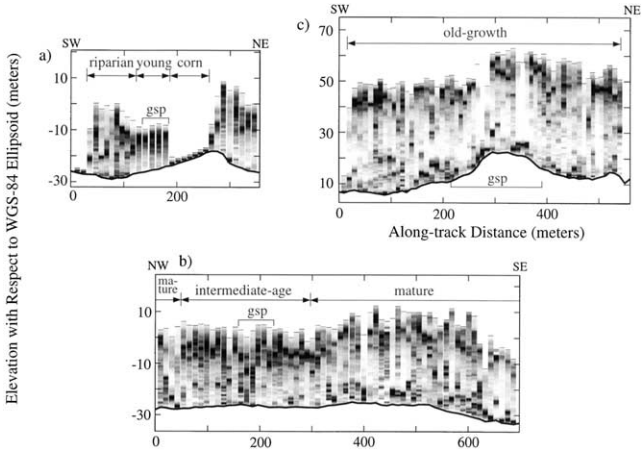

Fig. 7. SLICER canopy height profile transects across: (a) the young stand study site and adjacent stands; (b) the intermediate-age and mature stands within the SERC stem map (flight line 3); and (c) the old-growth stand, with ground sampling plot (gsp) locations indicated. Canopy height profiles are computed for individual laser shots along a single, cross-track footprint position within the SLICER swath. Darker gray shading corresponds to a greater fraction of plant area within a footprint. The width of the gray-scale columns corresponds to the diameter of each laser footprint. The solid, bold line and thin ticks indicate the elevation of the start of the ground return and the canopy top, respectively. Elevations are referenced to the WGS-84 ellipsoid, which is 33 m above mean sea level in the study region. Vertical exaggeration is 5:1.

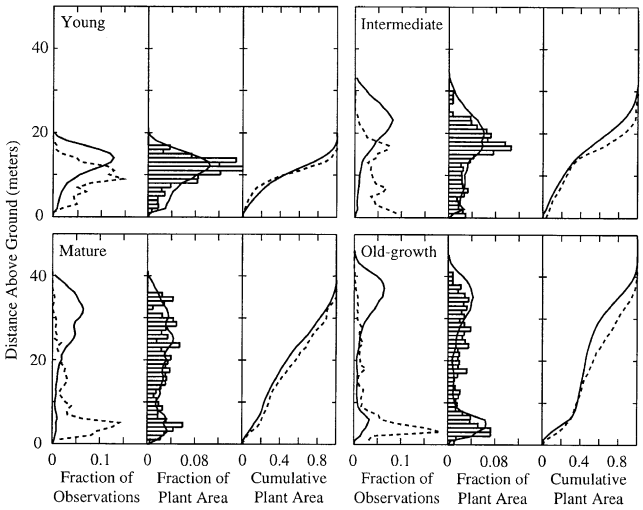

Fig. 8. Height distributions for untransformed observations (left panel), incremental canopy height profiles (center panel), and cumulative canopy height profiles (right panel) for the four study sites. SLICER results are shown as solid lines. Ground results are shown as dashed lines in the left and right panels, and as distribution bins in the center panel. Untransformed observations for the ground are the intercept sightings and for SLICER are the summed, above-ground waveform amplitudes, with each normalized. All results are binned at 1 m.

binning of the ground-based CHPs. Rightmost footprints in the SLICER swath were excluded due to low signal-to-noise, probably due to misalignment between the footprint scan pattern and the receiver field-of-view (Harding et al., 2000). Footprints lacking detectable ground returns at the mature site (located at the intersection of flight lines 2 and 4) were also excluded, along with the corresponding ground measurement points.

Comparisons of the SLICER and ground CHPs are shown in Fig. 8. Untransformed distributions of ground observed vertical interceptions and SLICER canopy return energy (left panels, Fig. 8) show each dataset's bias towards shorter distances due to the occlusion effect. In contrast, transformation of the data, via the MacArthur–Horn algorithm (center panels, Fig. 8), results in ground and SLICER CHPs whose general features are in agreement. The stand heights for both the ground and SLICER results increase in successional sequence from young to old-growth. For the shorter, unimodal young and intermediate-age stands, the vertical position of the single overstory peak is qualitatively in agreement. The height of the peaks (defined as the height at which the fraction of plant area in a height interval is at a maximum) in the ground and SLICER CHPs are within 3 m of each other. In addition, the decrease in relative plant area observed at heights both above and below the peak define slopes in the SLICER CHPs that are comparable to the ground CHPs. For the taller, bimodal mature and old-growth stands, the location and width of the understory peaks, a midstory decrease in the relative density of plant area, and the presence of a broad overstory are all similarly identified in the SLICER and ground CHPs.

Differences between the SLICER and ground measured CHPs do exist (Table 2). All of the SLICER CHPs are taller than the corresponding ground CHPs by between 7% and 12% (2 and 4 m). With one exception, the mean height of the SLICER CHPs was also higher by between 5% and 11% (0.9 and 2.2 m). The mean height of the SLICER CHP for the young plot was 9% (1.0 m) lower than the corresponding ground CHP. For the stands with a single clearly defined mode (young, intermediate-age), the SLICER CHPs result in a lower relative plant area at the peak height, underestimating this quantity by 33% in the young plot and 43% in the intermediate-age plot compared to the ground CHPs.

?twb=.4w>Assessing the SLICER to ground agreement of the two taller, bimodal stands (mature, old-growth) is more difficult. The overstory of the mature stand is very broad (25 m) and lacks a single well-defined peak in both the ground and SLICER CHPs. Instead, the overstory in both CHPs is composed of several small subpeaks. There is good qualitative agreement between the upper story depth and relative plant area amplitude in the ground and SLICER CHPs. The understory of the SLICER CHP has two subpeaks that bracket a single peak in the ground CHP, and SLICER underestimates the maximum relative plant area of the understory by 33% compared to the ground CHP. In the old-growth stand, the overstory in the ground CHP is significantly broader (25 m) and composed of multiple subpeaks compared to a single-peaked, narrower (15 m) overstory in the SLICER CHP. The difference in height between the SLICER and ground overstory maxima is about 5 m. The height of the SLICER CHP understory peak is about 1 m above the corresponding peak in the ground CHP, and SLICER estimates the maximum relative plant area of the understory to be 14% less than in the ground estimate.

The quantitative goodness-of-fit of these two measures of each stand's CHP has been evaluated in two ways. An R^2 test for each of the four sites demonstrates that the two

Table 2
Maximum and mean heights and height differences for ground observed and averaged SLICER CHPs from the four validation sites

	CHP maximum height				CHP mean height			
Site	Ground observed (m)	SLICER (m)	Ground minus SLICER (m)	Ground minus SLICER (%)	Ground observed (m)	SLICER (m)	Ground minus SLICER (m)	Ground minus SLICER (%)
Young	17	19	−2	−12	11.5	10.5	1.0	9
Intermediate	30	32	−2	−7	15.5	16.4	−0.9	−6
Mature	36	39	−3	−8	18.9	19.8	−0.9	−5
Old-growth	41	45	−4	−10	19.0	21.2	−2.2	−11

Table 3
Results of chi-square, uneven sample size, goodness-of-fit tests (95% confidence) used to determine if significant differences exist between averaged CHPs for each validation site made with subsampled and full SLICER waveforms

Site	Subsampled SLICER counts	Chi-square value	*P* value	Chi-square degree of freedom
Young	578	20.1	.27	17
Intermediate	974	29.9	.47	30
Mature	879	47.2	.12	37
Old-growth	1485	28.1	.96	44

distributions as a whole for each stand are correlated. R^2 values of .75, .52, .33, and .46 for the young, intermediate, mature, and old-growth stands, respectively, each have *P* values less than .0001. A more stringent chi-square goodness-of-fit test was also performed. In order to execute this test, which depends on the number of observations in each distribution, the CHP vectors had to be transformed into vectors of count data, rather than the normalized CHP distribution data. For the ground CHPs, vectors of counts were generated by multiplying the relative CHPs by the total number of ground observations. For the SLICER CHPs, a number of considerations had to be addressed before a sample size could be determined. The motivation for this determination of sample size is the higher statistical power, in the chi-square test, associated with a larger number of observations. If the number of observations is inflated, a higher probability of rejection will be obtained than is justified. The individual observation recorded by the SLICER system is the digitizer count, which represents an unknown number of individual received backscatter photons. Given the large number of digitizer-count observations (>4000 above background noise level), which are made over a 10-m footprint, it is likely that each observation represents a smaller area than is observed by the human operator making ground measurements. As a result, it is probable that individual SLICER and ground observations are not equivalent for statistical purposes.

To establish a statistically appropriate SLICER sample size, we applied a chi-square uneven sample size test to determine whether CHPs made using a subset of the SLICER digitizer counts, with a sample size equal to the number of ground observations for a site, were distinguishable from the site's average SLICER CHP created using the full waveforms. To create the subsampled CHPs, the ground returns were removed from each waveform and the digitizer counts were subsampled, pooled, and transformed to a CHP using the MacArthur–Horn method. The number of subsamples for each waveform was set so that, when pooled, they summed to the number of ground observations for that stand. No statistically significant differences between the subsampled and full-waveform CHPs were found using the chi-square test (Table 3). Therefore, subsampled waveforms were used in an even sample chi-square goodness-of-fit test between the ground and SLICER CHPs so as to not bias the results with an inflated sample size. However, even with the reduced SLICER sample size, the chi-square test indicates that there are statistically significant differences between the ground and SLICER CHPs for each stand (Table 4).

Table 4
Results of chi-square, even sample size, goodness-of-fit tests (95% confidence) used to determine if significant differences exist between ground CHPs and averaged, subsampled SLICER CHPs for each validation site

Site	Chi-square value	*P* value	Chi-square degree of freedom
Young	103.6	$<.0001$	17
Intermediate	215.0	$<.0001$	32
Mature	164.7	$<.0001$	39
Old-growth	396.1	$<.0001$	43

9. Discussion

The major characteristics of the SLICER and ground CHPs show good agreement for each stand, as indicated by the R^2 test and the similar depiction of upper and lower canopy modes (Fig. 8). Both also document the same changes in structure in the successional sequence from young to old-growth, closed-canopy, broadleaf forests. These general similarities between complimentary, but differently implemented, measurements of canopy intercept distances indicate that both the SLICER and ground CHPs depict basic attributes of these stands' vertical structure. Furthermore, the comparison of average SLICER CHPs at flight line intersections demonstrates that the laser altimeter results depict the canopy structure in a highly reproducible way. Despite the good general agreement between SLICER and ground CHPs, the failure to pass the chi-square test indicates that specific aspects of the CHPs exhibit statistically significant differences. The chi-square test is a stringent comparison because it can fail either through accumulated small differences between two vectors or due to a single large difference. The failure to pass this test speaks to differences at specific height increments rather than the overall similarity in form of the distributions that is indicated by the R^2 test and apparent in Fig. 8. In the following sections, we examine measurement and canopy factors that might give rise to the differences and evaluate how they might affect the comparison and the utility of the CHP method.

9.1. Measurement effects

Several factors cause the ground CHPs to be noisier and discontinuous compared to the SLICER CHPs (Table 5a). First, the ground measurements sample a small fraction of the canopy within the field plot (Fig. 3), whereas the SLICER illumination pattern fully samples the plot, although unevenly (Figs. 2 and 3). Second, the accuracy of the camera method for determining distances falls off rapidly with height (Lefsky, 1997), whereas the SLICER distances have constant accuracy. Third, the ground approach has only a small fraction of the observations per CHP compared to SLICER, resulting in a relative undersampling by the ground method. Fourth, the reduction of intercept observations at greater distances caused by occlusion (Fig. 8) yields SLICER and ground CHPs that are noisier low and high in the canopy, respectively. However, because the ground method consists of far fewer observations than SLICER, this effect is significantly more pronounced for the ground CHPs since the small number of overstory ground observations represents a great deal of leaf area following application of the MacArthur–Horn transform. Fifth, differences between the methods in the discreteness and dependence of the raw observations are also reflected in the smoothness of the transformed estimates of canopy structure. Because the SLICER waveform is sampled at an 11.12 cm vertical spacing that is significantly less than the instrument vertical resolution of approximately 2/3 of a meter, the returns are continuous and correlated over distances equal to the instrument resolution. Therefore, the derived CHPs are also continuous and somewhat smoothed. The ground intercept sightings are discrete and independent, yielding CHPs that can be discontinuous and stepped.

The overall effect of these measurement properties, yielding ground CHPs that are noisier and discontinuous compared to the SLICER CHPs, accounts, at least in part, for the observed chi-square statistical differences. The ground CHPs exhibit large variations in relative plant area from bin to bin compared to the smoother SLICER CHPs, especially higher in the canopy (Fig. 8). The few ground observations high in the canopy, and resulting empty CHP bins, account for the consistently lower maximum canopy height in the ground CHPs. The highest part of the canopy was not observed from the ground due to occlusion, whereas SLICER is most sensitive to plant area at the top of the canopy. It is likely that the SLICER observations, due to these sampling issues, are a more accurate estimate of the canopy vertical structure than are the ground observations.

9.2. Canopy effects

Departures from the assumptions of canopy uniformity cause height biases in the ground and SLICER CHPs (Table 5b). Clumping of foliage implies greater foliage-free distances than for the assumed horizontally random distribution. Therefore, laser energy will penetrate deeper into the canopy, whereas for the ground method, the upward distance to the first intercept will be longer causing SLICER CHPs to be biased high and the ground CHPs to be biased low for clumped canopies. Second, leaf inclinations for these canopies are not uniform as a function of height but, in fact, change from nearly flat (planophile) in the lower canopy to more vertical (erectophile) in the upper canopy (Parker, unpublished data). This change in leaf inclination yields fewer ground-observed intercepts and less SLICER backscatter energy per unit of total leaf area with increasing

Table 5

(a) Measurement properties of the ground and SLICER data and resulting effects on the noise level and continuity of the derived CHPs

Measurement property	Ground	SLICER	Effect on CHP (G = ground, S = SLICER)
Spatial sampling	point grid	complete illumination	G noisier than S
Distance accuracy	~5% to 10% of observation distance	constant, 11.12 cm	G noisier than S, especially high in canopy
Number of total observations	small	very large, oversampled	G noisier than S
Number of observations per CHP bin	fewer at larger distances	fewer at larger distances	G noisier higher, S noisier lower
Intrinsic smoothing	none, observations discrete and independent	pulse + detector = sliding window ~2/3 m in height	G discrete, stepped S continuous, smoothed

(b) Canopy properties potentially causing elevation biases in ground and SLICER CHPs

Canopy property	Ground	SLICER	Effect on CHP (G = ground, S = SLICER)
Nonrandom horizontal clumping	skewed to shorter distances	skewed to shorter distances	G biased low, S biased high
Leaf angle planophile to eroctophile upward	skewed to shorter distances	skewed to longer distances	G biased, low S biased low
Variability of canopy outer surface height	skewed to shorter distances	skewed to longer distances	G biased low, S biased low
Canopy vs. ground NIR reflectance ratio (C/G)	not applicable	actual C/G>2: actual C/G<2:	S biased low S biased high
Canopy NIR reflectance increases upward	not applicable	skewed to shorter distances	S biased high
Multiple scattering	not applicable	skewed to longer distances	S biased low

height in the canopy. Both methods are consequently biased in the same way to lower canopy heights.

Third, where there is much spatial variation in maximum canopy height ("rugosity" in the sense of Parker & Russ, in preparation; Weishampel et al., 2000), a too small weighting of distant foliage results in a ground CHP that is biased downwards. For the SLICER observation, the majority of the energy returned comes from the uppermost layer of the canopy. For canopies with planar outer surfaces, the return energy decreases due to occlusion in a horizontally uniform way. For canopies with a variable outer surface at the scale of the laser footprint, the return energy from the outer surface is distributed throughout the range of the upper canopy height distribution. Simulations demonstrate that this departure from uniformity biases the CHP in the direction of the mean plant area height. In these closed canopy cases where the mean canopy height is below the average height of the outermost canopy surface, the SLICER CHP is biased downwards. However, for the closed, planar deciduous canopies of this study, the effect is probably small.

Three canopy properties affect only the transformation of SLICER observations to CHPs (Table 5b). First, the transformation requires an estimate of the gap fraction that, for SLICER, depends on the canopy to ground NIR reflectance ratio, assumed to be two for the stands in this study. Underestimating this ratio causes the CHP to be biased low, whereas an overestimate causes a high bias. However, for high-closure canopies, the derivation of CHPs is relatively insensitive to errors in the assumed reflectance ratio. Fig. 9 shows only small departures between the average SLICER CHPs for the four study sites computed using ratios of 1, 2, and 4, corresponding to ground reflectance equal to, one-half, and one-quarter that of the canopy.

A second canopy property affecting the SLICER CHPs is the vertical distribution of canopy reflectance, which is assumed to be constant in the transformation method. Studies of broadleaf reflectance as a function of vertical position within canopies are rare, with the few results showing no significant within-species differences between upper and lower canopy leaves at NIR wavelengths (Demarez et al., 1999; Middleton, Walter-Shea, Mesarch, Chan, & Rusin, 1998). However, NIR leaf reflectance can change with height due to changes in species composition between stories; Middleton et al. (1998) document an upward increase in foliar NIR reflectance for three of four boreal forest stand types examined. A likely increase in the proportion of foliar vs. woody surfaces upward through canopies is also likely to cause canopy NIR reflectance to increase upward (e.g., Huemmrich & Goward, 1997). Plant area in SLICER CHPs will be biased high in cases where NIR reflectance increases upward.

Finally, any multiple scattering contribution to the waveform will cause the derived SLICER CHP to be biased low. The canopy undoubtedly causes significant scattering of the laser radiation, especially due to the high transmittance of deciduous leaves at NIR wavelengths. However, because the laser beam is highly collimated and the receiver has a very narrow field of view, we expect a relatively small fraction of the received backscatter returns to have been multiply scattered. Qualitative observation of individual, raw SLICER waveforms suggests that increased path length due to multiple scattering is minor, indicated by the presence of narrow vertical gaps within the canopy return where backscatter energy decreases to the background noise level and by the absence of a significant tail of multiply scattered return energy occurring later than the ground return. Furthermore, a comparison of modeled waveforms derived from high-resolution, small-footprint, first-return, laser altimeter data to waveforms acquired by LVIS reveals no discernable multiple scattering contribution to the backscatter signal from dense, multistoried rainforest canopies in Costa Rica (Blair & Hofton, 1999).

The result that the ground and SLICER methods yield similar CHPs indicates either that the instrument, sampling, and canopy interaction effects we have listed are all relatively small or in some way are negatively correlated and, for the most part, cancel each other. Because the offset of SLICER to ground CHP means increases upward as stand height increases (Table 2), it might be inferred that effects that bias the SLICER results upward and/or the ground downward predominate. However, examination of the ground to SLICER CHP comparisons (Fig. 8) shows that much, if not all, of the increasing offset in the means is due to the increasing underrepresentation of the upper canopy by the ground method as stand height increases. The underrepresentation of the upper canopy is likely caused by the difficulty in observing upper-canopy surfaces from the ground and the low total number of ground observations (Table 5a), rather than by errors introduced by the assumptions of canopy uniformity (Table 5b).

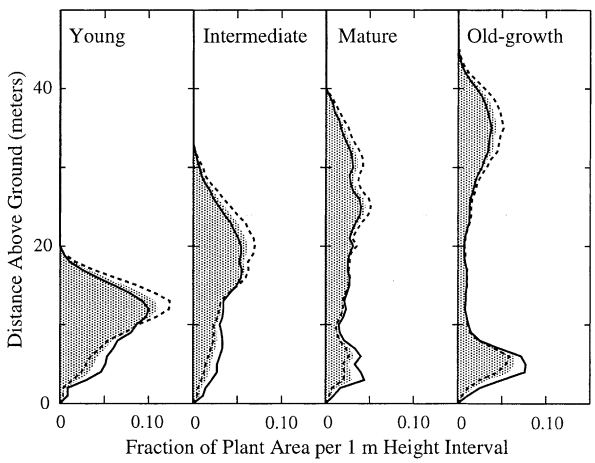

Fig. 9. Effect of ground return scale factor on SLICER canopy height profiles. Solid, shaded, and dashed distributions correspond to scale factors of 1, 2, and 4, respectively (equivalent to an average ground reflectance at 1064 nm and 0° phase angle equal to, one-half, and one-quarter that of the canopy).

9.3. Application of the results

There are some limitations in the domain over which these results can be applied and in the meaning that can be associated with the derived structure information. The current test has been restricted to closed-canopy (>90% closure), broadleaf forests. Direct application of the CHP methodology to other sorts of canopies may not be appropriate. Other canopies can depart more significantly from the assumptions of uniformity than the stands that we tested. In particular, open woodlands and stands of cone-shaped crowns strongly depart from the assumptions of random horizontal organization (no clumping) and uniform height of the canopy outer surface within the laser footprint. In addition, the CHP bias due to error in the ground reflectance scaling factor increases with decreasing canopy closure because of greater error introduced in the $[-\ln(1-\text{closure})]$ transformation weighting function. An error in scaling factor causes an error in closure that is larger, in an absolute sense, for open canopies compared to canopies with high closure.

It also must be remembered that the SLICER CHPs provide not the absolute height distribution of canopy surfaces, but the relative one; that is, the fraction of the total plant area within height intervals. It is not possible to predict the total amount of plant area from either the ground-based sightings or SLICER measurements (Aber, 1978; Lefsky, 1997). The total absolute plant area of a stand, obtained by other means such as leaf litter collections, must be combined with the SLICER relative CHP to yield an absolute height distribution. Furthermore, the SLICER return gives no information on the character of the reflecting surfaces in terms of the type of tissue (foliage or bark), its state (alive, stressed, or dead), or the species. The traditional foliage height profile (Aber, 1978), although manually intensive and, thus, spatially limited, can be used to provide important information on tissue type, state, and species (e.g., Brown & Parker, 1994) not achieved with the laser altimeter method.

10. Conclusions

The laser altimeter CHP methodology that we describe provides information about vertical structure that is closely related to similar measurements taken from the ground for the same portion of canopy: It reproduces the overall stature and the height of the principal modes in the distribution of plant area. In the same forest type, the method distinguishes different canopy structural types in a manner comparable to the ground observations, found from a comparison among developmental stages. Moreover, the method is reproducible: Repeat measurements of the same locations give essentially the same vertical distributions. Together, these characteristics validate a remote sensing approach that rapidly obtains information of considerable ecological value about the organization of forest canopies, a major component of the biosphere.

Although the laser altimeter and ground-based measures of canopy vertical structure similarly characterize the structural variations between the four stands studied, there are statistically significant differences between the CHPs for individual stands. These differences are in part a consequence of the attributes of the data, with SLICER resulting in smooth, continuous, very well-sampled distributions and ground observations resulting in stepped, discrete, less well-sampled distributions. This is especially the case high in the canopy where ground-based sightings are rare, typically resulting in an underestimate of canopy surface area and height as compared to the SLICER results. Departure from the assumptions regarding canopy properties used to transform raw observations to surface area height distributions may also lead to differences between the SLICER and ground results. In particular, departures from the assumption of horizontal randomness caused by clumping bias the distributions toward the observer, upward for SLICER and downward for ground-based CHPs, and an upward increase in canopy NIR reflectance would bias the SLICER CHP upward.

The highly resolved and reproducible observations of canopy structure achieved by laser altimeter waveform observations provides a new method to assess important aspects of spatial and temporal variation in vegetation, including gap structure, stand complexity, and structural diversity. The footprint size of SLICER (nominally 10 m) was chosen to reflect the size of the characteristic canopy element: It is large enough to capture the local maximum height of an assemblage of tree crowns and yet small enough to reliably differentiate ground and canopy contributions to the waveform. This is an important scale in forest dynamics in mature stands because it is the typical size of the canopy hole produced when a tree falls. Studies of the structural variation of vegetation at spatial scales on the order of 10 m have not, to date, been possible with traditional field or remote sensing methods.

Acknowledgments

This work was supported by the Terrestrial Ecology Program of NASA's Earth Science Enterprise, the NASA Global Change Fellowship program, and the Smithsonian Environmental Sciences Program. The work was performed at NASA's Goddard Space Flight Center, the University of Virginia, the USDA Forest Service Pacific-Northwest Research Station, and the SERC. Development of the SLICER instrument was supported by NASA's Solid Earth Science Program and the Goddard Director's Discretionary Fund. SLICER data sets available for public distribution are documented at http://denali.gsfc.nasa.gov/lapf. We thank David Rabine and Barry Coyle for operation of the SLICER instrument and Earl Frederick and Bill Krabill for assistance

in GPS operations. The Aircraft Programs Branch at Goddard's Wallops Flight Facility conducted the aircraft flight operations for the SLICER data acquisition, and Wayne Wright provided the flight navigation software. Michelle Hofton made improvements to the geolocation software developed by one of us (Blair) and Melanie Taylor and Kathy Still applied the SLICER geolocation processing. George Rasberry and Donna Tibbs conducted the ground-based foliage profile measurements. Dr. Lefsky also thanks Drs. H.H. Shugart, B.P. Hayden, J.H. Porter, and W.B. Cohen for their assistance. We thank Jon Ranson, Jim Smith, and two anonymous reviewers for constructive comments that improved the manuscript.

References

Aber, J. D. (1978). A method for estimating foliage-height profiles in broad-leaved forest. *Journal of Ecology*, *67*, 35–40.

Aber, J. D. (1979). Foliage-height profiles and succession in Northern Hardwood forest. *Ecology*, *60*, 18–23.

Aber, J. D., Pastor, J. H., & Melillo, J. M. (1982). Changes in forest canopy structure along a site quality gradient in southern Wisconsin. *American Midland Naturalist*, *108*, 256–265.

Aldred, A., & Bonner, G. (1985). Application of airborne lasers to forest surveys, Petawawa National Forestry Institute, Canadian Forestry Service, Information Report PI-X-51, 61 pp.

Askne, J. I. H., Dammert, P. B. G., Ulander, L. M. H., & Smith, G. (1997). C-band repeat-pass interferometric SAR observations of the forest. *IEEE Transactions on Geoscience and Remote Sensing*, *35*, 25–35.

Blair, J. B., Coyle, D. B., Bufton, J. L., & Harding, D. J. (1994). Optimization of an airborne laser altimeter for remote sensing of vegetation and tree canopies. In: *Proceedings of the international geoscience and remote sensing symposium '94* (pp. 939–941). Piscataway, NJ: IEEE Geosci. Rem. Sens. Soc.

Blair, J. B., & Hofton, M. A. (1999). Modeling laser altimeter return waveforms over complex vegetation using high-resolution elevation data. *Geophysical Research Letters*, *26*, 2509–2512.

Blair, J. B., Rabine, D. L., & Hofton, M. A. (1999). The Laser Vegetation Imaging Sensor (LVIS): a medium-altitude, digitization-only, airborne laser altimeter for mapping vegetation and topography. *ISPRS Journal of Photogrammetry and Remote Sensing*, *54*, 115–122.

Brown, M. J., & Parker, G. G. (1994). Canopy light transmittance in an chronosequence of mixed-species deciduous forests. *Canadian Journal of Forest Research*, *24*, 1694–1703.

Brush, G. S., Lenk, C., & Smith, J. (1980). The natural forest of Maryland: an explanation of the vegetation map of Maryland. *Ecological Monographs*, *50*, 77–92.

Bufton, J. L. (1989). Laser altimetry measurements from aircraft and spacecraft. *Proceedings of the IEEE*, *77*, 463–477.

Bufton, J. L., Garvin, J. B., Cavanaugh, J. F., Ramos-Izquierdo, L., Clem, T. D., & Krabill, W. B. (1991). Airborne lidar for profiling of surface topography. *Optical Engineering*, *30*, 72–78.

Carabajal, C. C., Harding, D. J., Luthcke, S. B., Fong, W., Rowton, S. C., & Frawley, J. J. (1999). Processing of Shuttle Laser Altimeter range and return pulse data in support of SLA-02. *International Archives of Photogrammetry and Remote Sensing*, *32* (3W14), 65–72.

Chen, J. M., & Cihlar, J. (1996). Retrieving leaf area index of boreal conifer forests using Landsat TM images. *Remote Sensing of Environment*, *55*, 153–162.

Cloude, S. R., & Papathanassiou, K. P. (1998). Polarimetric SAR interferometry. *IEEE Transactions on Geoscience Remote Sensing*, *36*, 1551–1565.

Dammert, P. B. G., & Askne, J. (1998). Interferometric tree height observations in boreal forests with SAR interferometry. In: *Proceedings of the international geosciences and remote sensing symposium '98* (pp. 1363–1366). Piscataway, NJ: IEEE Geosci. Rem. Sens. Soc.

Demarez, V., Gastellu-Etchegorry, J. P., Mougin, E., Marty, G., Proisy, C., Dufrene, E., & Le Dantec, V. (1999). Seasonal variation of leaf chlorophyll content of a temperate forest. Inversion of the PROSPECT model. *International Journal of Remote Sensing*, *20*, 879–894.

Dobson, M. C., Ulaby, F. T., Pierce, L. E., Sharik, T. L., Bergen, K. M., Kellndorfer, J., Kendra, J. R., Li, E., Lin, Y. C., Nashashibi, A., Sarabandi, K., & Siqueira, P. (1995). Estimation of forest biophysical characteristics in northern Michigan with SIR-C/XSAR. *IEEE Transactions on Geoscience and Remote Sensing*, *33*, 877–895.

Drake, J. B., & Weishampel, J. F. (2000). Multifractal analysis of canopy height measures in a longleaf pine savanna. *Forest Ecology and Management*, *128*, 121–127.

Dubayah, R., Blair, J. B., Bufton, J. L., Clark, D. B., JaJa, J., Knox, R., Luthcke, S. B., Prince, S., & Weishampel, J. (1997). The Vegetation Canopy Lidar mission. In: *Proceedings of land satellite information in the next decade: II. Sources and applications* (pp. 100–112). Bethesda, MD: Am. Soc. Photogram. Remote Sens.

Eyre, F. H. (Ed.). (1980). *Forest cover types of the United States and Canada*. Washington, DC: Society of American Foresters.

Garvin, J., Bufton, J., Blair, J., Harding, D., Luthcke, S., Frawley, J., & Rowlands, D. (1998). Observations of the Earth's topography from the Shuttle Laser Altimeter (SLA): laser-pulse echo-recovery measurements of terrestrial surfaces. *Physics and Chemistry of the Earth*, *23*, 1053–1068.

Hagberg, J. O., Ulander, L. M. H., & Askne, J. (1995). Repeat-pass SAR interferometry over forested terrain. *IEEE Transactions on Geoscience and Remote Sensing*, *33*, 331–340.

Harding, D. J., Blair, J. B., Rabine, D. L., & Still, K. L. (2000). SLICER airborne laser altimeter characterization of canopy structure and subcanopy topography for the BOREAS northern and southern study regions: instrument and data product description. In F. Hall & J. Nickeson (Eds.), *Technical report series on the boreal ecosystem–atmosphere study (BOREAS): Remote Sensing Sciences Group*. NASA/TM-2000-209891.

Hedman, C. W., & Binkley, D. (1988). Canopy profiles of some Piedmont hardwood forests. *Canadian Journal of Forest Research*, *18*, 1090–1093.

Hofton, M. A., Blair, J. B., Minster, J.-B., Ridgway, J. R., Williams, N. P., Bufton, J. L., & Rabine, D. L. (2000). An airborne scanning laser altimetry survey of Long Valley, California. *International Journal of Remote Sensing*, *21*, 2413–2437.

Hofton, M. A., Minster, J. B., & Blair, J. B. (2000). Decomposition of laser altimeter waveforms. *IEEE Transactions on Geoscience and Remote Sensing*, *38*, 1989–1996.

Huemmrich, K. F., & Goward, S. N. (1997). Vegetation canopy PAR absorptance and NDVI: an assessment for ten tree species with the SAIL model. *Remote Sensing of Environment*, *61*, 254–269.

Imhoff, M. L. (1995). Radar backscatter and biomass saturation — ramifications for global biomass inventory. *IEEE Transactions on Geoscience and Remote Sensing*, *33*, 511–518.

Lathrop, R. G., & Pierce, L. L. (1991). Ground-based canopy transmittance and satellite remotely sensed measurements for estimation of coniferous forest canopy structure. *Remote Sensing of Environment*, *36*, 179–188.

Lefsky, M., Cohen, W., Acker, S., Parker, G., Spies, T., & Harding, D. (1999). Lidar remote sensing of biophysical properties and canopy structure of forests of Douglas-fir and western hemlock. *Remote Sensing of Environment*, *70*, 339–361.

Lefsky, M. A. (1997). Application of lidar remote sensing to the estimation of forest canopy and stand structure. PhD dissertation, University of Virginia, Charlottesville, VA.

Lefsky, M. A., Cohen, W. B., Harding, D. J., & Parker, G. G. (in review). Lidar remote sensing for ecosystem studies. *Biosciences*.

Lefsky, M. A., Harding, D. J., Cohen, W. B., Parker, G. G., & Shugart, H.

B. (1999). Lidar remote sensing of forest basal area and biomass: application and theory. *Remote Sensing of Environment*, *67*, 83–98.

Le Toan, T., Beaudoin, A., Riom, J., & Guyon, D. (1992). Relating forest biomass to SAR data. *IEEE Transactions on Geoscience and Remote Sensing*, *30*, 403–411.

MacArthur, R. H., & Horn, H. S. (1969). Foliage profiles by vertical measurements. *Ecology*, *50*, 802–804.

Means, J. E., Acker, S. A., Harding, D. J., Blair, J. B., Lefsky, M. J., Cohen, W. B., Harmon, M. E., & Mckee, W. A. (1999). Use of large-footprint scanning airborne lidar to estimate forest stand characteristics in the western Cascades of Oregon. *Remote Sensing of Environment*, *67*, 298–308.

Middleton, E. M., Walter-Shea, E. A., Mesarch, M. A., Chan, S. S., & Rusin, R. J. (1998). Optical properties of canopy elements in black spruce, jack pine, and aspen stands in Saskatchewan, Canada. *Canadian Journal of Remote Sensing*, *24*, 169–186.

Nemani, R. R., Pierce, L., Running, S., & Band, L. (1993). Forest ecosystem processes at the watershed scale: sensitivity to remotely-sensed leaf area index estimates. *International Journal of Remote Sensing*, *14*, 2519–2534.

Nilsson, M. (1996). Estimation of tree heights and stand volume using an airborne lidar system. *Remote Sensing of Environment*, *56*, 1–7.

Parker, G. G. (1995). Structure and microclimate of forest canopies. In: M. Lowman, & N. Nadkarni (Eds.), *Forest canopies — a review of research on a biological frontier* (pp. 73–106). San Diego, CA: Academic Press.

Parker, G. G., Lefsky, M. A., & Harding, D. J. (2001). Light transmittance in forest canopies determined using airborne laser altimetry and in-canopy quantum measurements. *Remote Sensing of Environment, 73,* 298–310.

Parker, G. G., O'Neill, J. P., & Higman, D. (1989). Vertical profile and canopy organization in a mixed deciduous forest. *Vegetation*, *85*, 1–11.

Parker, G. G., & Russ, M. E. (in preparation). The canopy surface and stand development: assessing forest canopy structure and complexity with near-surface altimetry. *Ecology.*

Parker, G. G., & Tibbs, D. J. (in review). Leaf area phenology of a deciduous forest canopy. *Forest Science*.

Ranson, K. J., Sun, G., Weishampel, J. F., & Knox, R. G. (1997). Forest biomass from combined ecosystem and radar backscatter modeling. *Remote Sensing of Environment*, *59*, 118–133.

Sader, S. A., & Joyce, A. T. (1990). Remote sensing of tropical forests: an overview of research and applications using non-photographic sensors. *Photogrammetric Engineering and Remote Sensing*, *56*, 1343–1351.

Spanner, M. A., Peterson, D. L., & Running, S. W. (1990). Remote sensing of temperate coniferous forest leaf area index: the influence of canopy closure, understory vegetation and background relectance. *International Journal of Remote Sensing*, *11*, 95–111.

Sun, G., & Ranson, K. J. (1995). A three-dimensional radar backscatter model of forest canopies. *IEEE Transactions on Geoscience and Remote Sensing*, *33*, 372–382.

Treuhaft, R. N., Madsen, S. E., Moghaddam, M., & Vanzyl, J. J. (1996). Vegetation characteristics and underlying topography from interferometric radar. *Radio Science*, *31*, 1449–1485.

Treuhaft, R. N., & Moghaddam, M. (1998). A unified analysis of radar interferometry and polarimetry for the estimation of forest parameters. In: *Proceedings of the international geoscience and remote sensing symposium '98* (pp. 1373–1375). Piscataway, NJ: IEEE Geosci. Rem. Sens. Soc.

Ulaby, F. T., Moore, R. K., & Fung, A. K. (1986). *Microwave remote sensing: active to passive: vol. III. From theory to applications*. Norwood, MA: Artech House.

Vaughn, C. R., Bufton, J. L., Krabill, W. B., & Rabine, D. (1996). Georeferencing of airborne laser altimeter measurements. *International Journal of Remote Sensing*, *17*, 2185–2200.

Weishampel, J. F., Blair, J. B., Knox, R. G., Dubayah, R., & Clark, D. B. (2000). Volumetric lidar return patterns from an old-growth tropical rainforest canopy. *International Journal of Remote Sensing*, *21*, 409–415.

Weishampel, J. F., Ranson, K. J., & Harding, D. J. (1996). Remote sensing of forest canopies. *Selbyana*, *17*, 6–14.